

## Determination of electron temperature in low-pressure plasmas by means of optical emission spectroscopy

*S. Mitic\**, *B. A. Klumov\*<sup>+</sup>*, *M. Y. Pustynnik\**, *G. E. Morfill\**

*\*Max-Planck-Institut für Extraterrestrische Physik, D-85740 Garching, Germany*

*<sup>+</sup>Joint Institute for High Temperatures RAS, 125412 Moscow, Russia*

Submitted 20 January 2010

Resubmitted 3 February 2010

A simple model, allowing to determine the electron temperature in a steady-state low-pressure plasma, is proposed. The model makes use of optical cross-sections and therefore takes into account direct and cascade excitation from ground and metastable states. Spectroscopic data from Mitic et al. (New J. Phys. 11, 083020 (2009)) are used to illustrate the performance of the method.

Optical emission spectroscopy is a widely used non-intrusive method of plasma diagnostics [1]. The advantage of low-pressure plasmas is that the excited levels except for long-living metastables decay only radiatively. In equilibrium decay rate should equal the excitation rate, including the excitation from ground and metastable states. Excitation rate, however, is proportional to the electron density. Therefore, the ratio of line intensities, emitted from the same volume, depends only on the excitation cross-sections and the electron energy distribution function (EEDF). Provided the excitation cross-sections are known and the shape of the EEDF can be hypothesized, parameters of the EEDF (in the simplest case of the Maxwellian EEDF, on which we concentrate ourselves further in the article, electron temperature  $T_e$ ) can be determined [2–5]. We should note, that a necessary instrumental condition for this kind of measurement is that a spectroscopic system is at least relatively calibrated.

Here we propose a method, that allows to determine the parameters of the EEDF, using the ratio of intensities of the same spectral line, measured from two different, but equal volumes of the plasma. This cancels the necessity of the relative calibration.

**Model.** Our assumptions are the following:

1) plasma is optically thin along any direction for the observed spectral lines; resonant vacuum UV radiation, however, may be trapped;

2) the shape of the EEDF in both volumes is Maxwellian with temperatures  $T_{e,1}$  and  $T_{e,2}$ ;

3) in both volumes the radiative levels are populated by (i) direct electron impact excitation of ground and metastable states and (ii) cascades from upper lying levels;

4) in both volumes depopulation of the levels is only by the radiative decay;

5) within each of the volumes the plasma is uniform.

In our consideration we use the optical cross-sections [7, 8] for the ground and metastable states. The advantage of optical cross-sections versus direct excitation cross-sections is that the optical cross-sections connect electron flux in the plasma with the photon flux it produces in a specific transition by exciting ground state or metastable atoms: they automatically account for such issues as the population of the upper level of the transition from cascades, radiation trapping, multiple decay channels of the upper level.

The measured intensity of a spectral line can be expressed as follows:

$$I_{ij} = C_{ij} h\nu_{ij} n_e \sum_s n_s k_{ij}^s, \quad (1)$$

where  $C_{ij}$  is the sensitivity of the detector for the photons with energy  $h\nu_{ij}$ ,  $n_e$  electron density,  $n_s$  is the density of the state  $s$ , excitation from which is considered (i.e. either ground state  $g$  or one of the metastable states) and  $k_{ij}^s$  is the emission rate in the transition  $i \rightarrow j$  due to the excitation from the state  $s$ .

$$k_{ij}^s = \int_0^\infty v \sigma_{ij}^s(v) f(v) dv, \quad (2)$$

where  $v$  is the electron velocity,  $\sigma_{ij}^s(v)$  is the optical cross-section for the state  $s$  and transition  $i \rightarrow j$ ,  $f(v)$  is the electron velocity distribution function. In the case of Maxwellian EEDF  $k_{ij}^s$  depends only on the electron temperature.

Suppose  $I_{ij,1}$  and  $I_{ij,2}$  are the intensities measured from the two different volumes of the plasma. Their ratio can then be expressed as follows:

$$E_{ij} \left( T_{e,1}, T_{e,2}, \frac{n_{e,1}}{n_{e,2}} \right) = \frac{I_{ij,1}}{I_{ij,2}} = \frac{n_{e,1}}{n_{e,2}} \frac{\sum_s n_{s,1} k_{ij}^s(T_{e,1})}{\sum_s n_{s,2} k_{ij}^s(T_{e,2})}. \quad (3)$$

$n_{e,1}$ ,  $n_{e,2}$  are here the electron densities and  $n_{s,1}$ ,  $n_{s,2}$  are the densities of long-living states of argon in the two volumes respectively. Ratio  $E_{ij}$  depends on both electron temperatures and ratio of electron densities  $n_{e,1}/n_{e,2}$ . Let us consider three different transitions  $\alpha, \beta$  and  $\gamma$ . Then, using two transitions we can define a quantity  $F$ , which is totally independent of electron densities:

$$F_{\alpha,\beta}(T_{e,1}, T_{e,2}) = \frac{E_{\alpha}(T_{e,1}, T_{e,2}, n_{e,1}/n_{e,2})}{E_{\beta}(T_{e,1}, T_{e,2}, n_{e,1}/n_{e,2})} = \frac{I_{\alpha,1}/I_{\alpha,2}}{I_{\beta,1}/I_{\beta,2}}. \quad (4)$$

Adding the third transition allows us to determine  $T_{e,1}$  and  $T_{e,2}$ , solving the following system of equations:

$$F_{\alpha,\beta}(T_{e,1}, T_{e,2}) - \frac{I_{\alpha,1}/I_{\alpha,2}}{I_{\beta,1}/I_{\beta,2}} = 0, \quad (5)$$

$$F_{\beta,\gamma}(T_{e,1}, T_{e,2}) - \frac{I_{\beta,1}/I_{\beta,2}}{I_{\gamma,1}/I_{\gamma,2}} = 0. \quad (6)$$

In principle, a system, involving more transitions, can be constructed and further solved by, e.g. using the mean least squares method.

We concentrate on the Maxwellian EEDF only for simplicity. Taking more spectral lines into consideration would allow to extend this method for the case of a more complicated EEDF.

**Experiment.** As an example we use the spectroscopic data, obtained in a previous [9] experiment. In this experiment the plasma is generated in a PK3+ chamber, which is the heart of a International-Space-Station-based complex plasma laboratory [10]. Briefly, PK3+ is a symmetrically driven parallel-plate 13.56 MHz discharge with the disc-shaped electrodes of 6 cm in diameter and 3 cm gap. Experiments were carried out in argon buffer gas at working pressure of 60 Pa, RF voltage of about 20 V peak-to-peak and power of 0.2 W. Spectra were recorded using a Hamamatsu Minispectrometer Module TG series, by collecting column of light parallel to the electrodes through a collimator into the optic fiber, which could be moved vertically by a translation stage in order to obtain axial profile of the emission.

Two types of measurements were done: one in pure argon plasma and the other with a cloud of melamine-formaldehyde monodisperse spheres of 2.55  $\mu\text{m}$  diameter, levitating in it. Under gravity conditions these microparticles concentrated themselves in the vicinity of the bottom electrode. Typical number density of microparticles, levitating in the plasma, was always of the order of  $10^{11} \text{ m}^{-3}$ .

Optical cross-section for the spectral lines of argon are known for the excitation from the ground state [11] as well as from the metastable states  $1s_5$  and  $1s_3$  [12].

The input parameters of the method, described above, are the densities of the long-living argon states, i.e.  $n_g$ ,  $n_{1s_5}$ ,  $n_{1s_3}$  and intensities of spectral lines. Since the ionization degree is small,  $n_g$  can be determined from the argon pressure. Metastable densities are measured by a single-mirror method [13], which is corrected for the presence of a microparticle cloud in a plasma [9].

Use of the intensities of the spectral lines, measured in Ref. [9] requires an important physical comment. In Ref. [9] it was revealed, that self-absorption (together with the extinction in case of complex plasmas) is important. In fact, measurement of  $1s$  states, performed in Ref. [9], was possible due to the relatively large self-absorption. We assumed, however, that for the spectral lines  $\alpha, \beta$  and  $\gamma$  the plasma is optically thin. This means, that the measured intensities of the spectral lines cannot be simply substituted into eqs. (5) and (6). To get rid of the self-absorption and extinction the so-called escape factor should be used [14]. Since our detector observes a thin column of plasma, it is not difficult to connect the measured intensity  $I_{ij}^{\text{meas}}$  to the "local" intensity  $I_{ij}^{\text{loc}}$ , i.e. to the locally emitted photon flux [9] for a Doppler-broadened line:

$$I_{ij}^{\text{loc}} = I_{ij}^{\text{meas}} \left( \frac{1}{\sqrt{\pi}} \int_{-\infty}^{\infty} \frac{e^{-\omega^2}}{\tau_{ij}^{\text{pl}}(0)e^{-\omega^2} + \ln(K_{ij}^{\text{d}})} \times \left( 1 - \frac{\exp(-\tau_{ij}^{\text{pl}}(0)e^{-\omega^2})}{K_{ij}^{\text{d}}} \right) d\omega \right)^{-1}. \quad (7)$$

Here  $\tau_{ij}^{\text{pl}}(0)$  is the optical thickness in the center of the spectral line and  $K_{ij}^{\text{d}}$  is the microparticle-caused attenuation of the plasma light. Both values are determined in Ref. [9]. Intensities of the following three spectral lines of argon, measured by a spectrometer, are used as  $I_{ij}^{\text{meas}}$ : 794.8, 826.4 and 706.7 nm (corresponding transitions  $\alpha = \{2p_4 \rightarrow 1s_3\}$ ,  $\beta = \{2p_2 \rightarrow 1s_2\}$  and  $\gamma = \{2p_3 \rightarrow 1s_5\}$ ). These measured intensities are recalculated into "local" intensities using Eq. (7) and then substituted into Eqs. (5) and (6).

We should note, that Eq. 1 does not take into account self-absorption as a populating mechanism for the level  $i$ . This would lead to the necessity of considering the radiation transfer in the discharge, which significantly complicates the problem.

Optical cross-sections depend on the escape factor for the vacuum UV resonant photons [11], i.e. background gas pressure and dimensions of the setup. Dimensions of PK3+ chamber are comparable to those of the chamber, in which the optical cross-sections were measured. The measurements of the optical cross-sections were performed in the range of pressures of  $10^{-1} - 1$  Pa. In two limiting cases of small pressure and

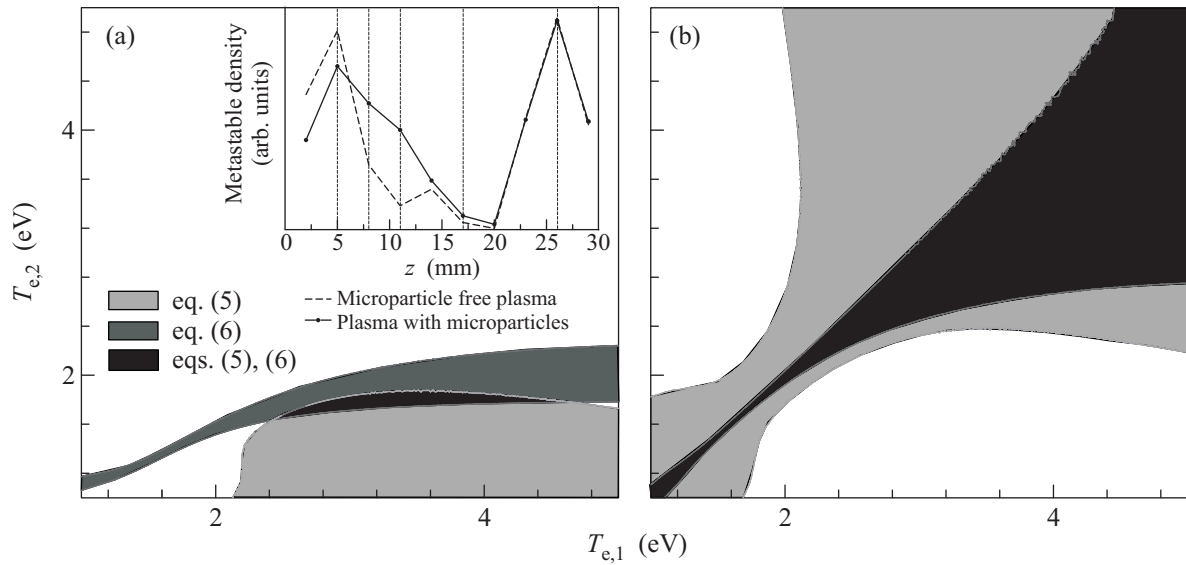


Fig.1. Solution of eqs. (5) and (6) for the points in microparticle-free plasma at the argon pressure of 60 Pa and RF power of 0.2 W [9] with  $\delta F = \pm 0.05$ : (a) index 1 corresponds to the vertical position  $z = 5$  mm (peak of emission), index 2 – to  $z = 11$  mm (minimum of the emission); in the inset the axial distributions of the number density of metastable atoms are presented; vertical dotted lines indicate the positions, at which the electron temperatures are evaluated; (b) index 1 –  $z = 5$  mm (peak of emission), index 2 –  $z = 26$  mm (symmetric peak of emission). Evidently, the temperatures are much better determined if the two points with significantly different parameters are considered

high pressure the optical cross-section is constant since the escape factor tends in these cases to unity and zero respectively. At high pressures the pressure dependence of the cross-sections start to saturate at about 0.66 Pa (5 mTorr). Therefore, at our working pressure this dependence is with a good guarantee saturated. Therefore, we used the optical cross-sections, measured for the pressure of 0.66 Pa.

In an ideal case solution of each of the eqs. (5) and (6) can be represented as a curve on the  $(T_{e,1}, T_{e,2})$  plane. The intersection of these curves would yield the solution of the system and therefore, values of temperatures. However, in reality the line intensities are measured with a finite uncertainty, which results in the uncertainty of the function  $F$ . For the solution of (5) and (6) this would mean, that instead of exact values of the temperatures, only a range, in which the temperatures may lie at a given experimental uncertainty  $\delta F$ , can be determined. In our experiments  $F_{\alpha,\beta}$  and  $F_{\beta,\gamma}$  varied roughly between 0.9 and 1.1.

**Results for microparticle-free plasma.** Further we provide several examples of the solution of the system of (5) and (6). Due to large errors in the obtained temperatures, we cannot pretend on any quantitiveness of our measurements. Therefore, the examples below are used just to demonstrate the performance of the method and to give the ideas of how the method can be applied to the experimental data.

First group of examples, in which we consider two different points of the same microparticle-free discharge, is presented in Fig.1. Obviously, the temperatures are much better determined in the case, when the two points with significantly different conditions are taken. From Fig.1a we have for  $T_{e,1} = 2.5 \div 4.7$  eV at the height  $z = 5$  mm over the bottom electrode of the discharge and  $T_{e,2} = 1.6 \div 1.8$  eV at  $z = 11$  mm, i.e.  $T_{e,1} > T_{e,2}$ , which is expected since points 1 and 2 correspond to hump and dip of the emission respectively. At the same time in Fig.1b the intersection of the solutions of (5) and (6) covers the entire considered range of temperatures. It is therefore practically impossible to draw any quantitative information about the temperatures. However, the line  $T_{e,1} = T_{e,2}$  lies inside the solution area, which is expected, since in Fig.1b symmetric points of the discharge are considered.

**Estimations of the influence of microparticles on  $T_e$ .** This method can be also used to evaluate the influence of the the presence of microparticles on the electron temperature by substituting into (5) and (6) the intensities, measured at the same  $z$  in microparticle-free plasma and in plasma, containing a microparticle cloud (Fig.2). Previously [9] it has been revealed, that the cloud of microparticles produces a significant non-local influence on the distribution of the densities of 1s states of argon in an RF discharge. For the following consideration we define the electron temperature in a

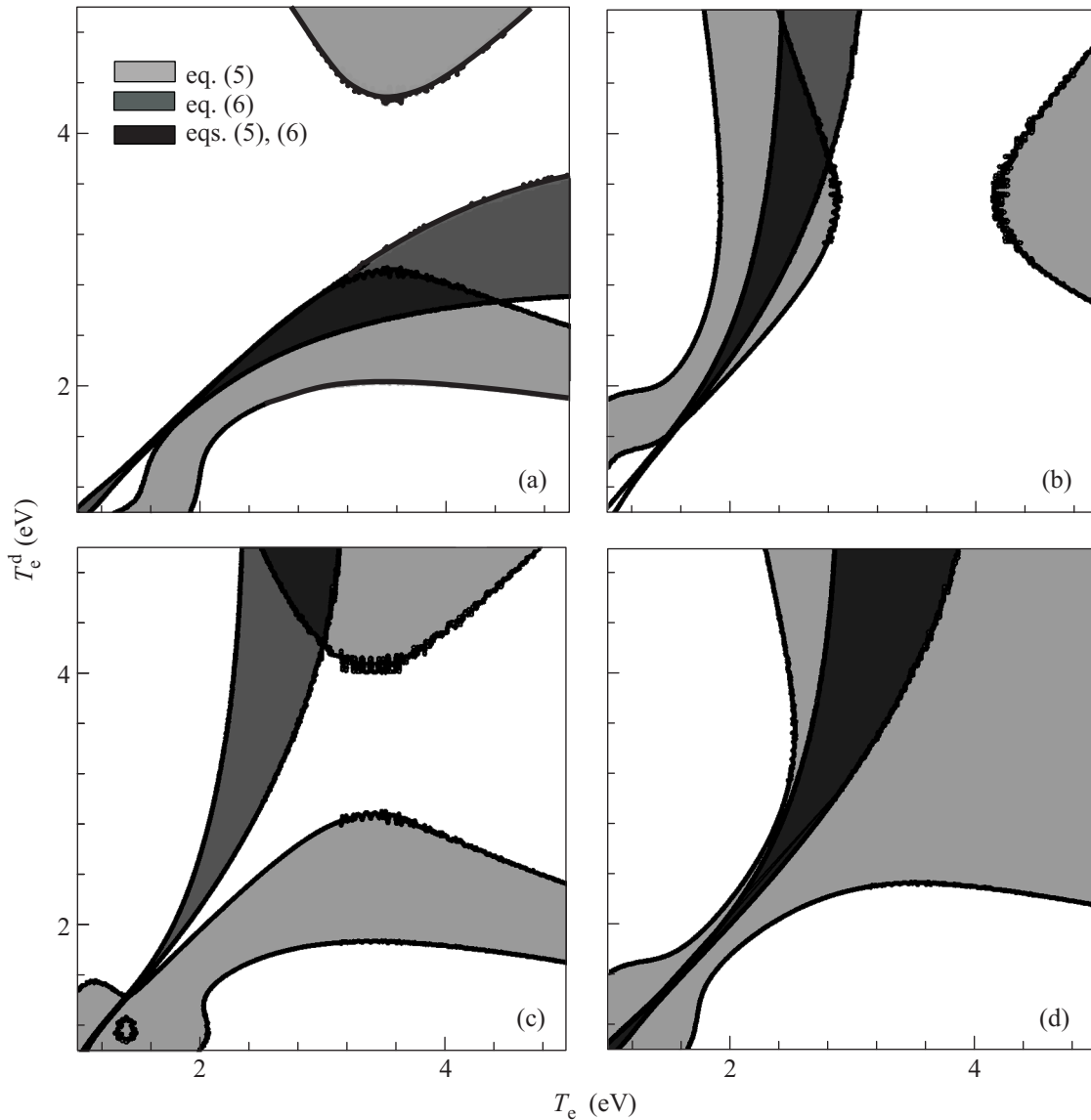


Fig.2. Solution of eqs. (5) and (6) for the points in the plasma at the argon pressure of 60 Pa and RF power of 0.2 W [9] with  $\delta F = \pm 0.02$ . Indices 1 and 2 correspond to the same vertical position  $z$  in microparticle-free plasma and plasma with microparticles respectively;  $T_e \equiv T_{e,1}$ ,  $T_e^d \equiv T_{e,2}$ . (a)  $z = 5$  mm, presence of microparticles decreases the densities of  $1s$  states; (b)  $z = 8$  mm, presence of microparticles increases the densities of  $1s$  states; (c)  $z = 17$  mm, presence of microparticles practically does not affect the densities of  $1s$  states; (d)  $z = 26$  mm, presence of microparticles practically does not affect the densities of  $1s$  states. Vertical positions for (a) and (b) are inside the microparticle cloud, whereas for (c) and (d) outside. For (d) the density of  $1s$  states is significantly higher, than that for (c).  $T_e$  exhibits much larger upper limit than  $T_e^d$  in (a) and vice versa in (b), which is in accord with the previously observed effect of microparticles on the densities of  $1s$  states of argon. For (c) and (d) effect of microparticles is negligibly small and therefore, determination of the temperatures is not possible

microparticle-free plasma  $T_e \equiv T_{e,1}$  and electron temperature in a plasma, containing a microparticle cloud,  $T_e^d \equiv T_{e,2}$ . At  $z = 5$  mm (Fig.2a) the upper limit of  $T_e$  is 4.4 eV, i.e. significantly larger than that of  $T_e^d$  (2.8 eV). In accord with this, presence of microparticles leads to decrease of the densities of  $1s$  states at this height. Situation is opposite at  $z = 8$  mm (Fig.2b), where the upper

limit of  $T_e^d$  is higher and the densities of  $1s$  states increase in presence of microparticles. At heights  $z$  of 17 and 26 mm (Fig.2c and Fig.2d respectively), where the influence of microparticles is small,  $T_e$  and  $T_e^d$  can hardly be determined.

In conclusion, we presented a spectroscopic method, allowing to evaluate (in the assumption of a Maxwellian

EEDF) the electron temperature in a low-pressure plasma. The input parameters of the method are the experimentally measured intensities of spectral lines and densities of metastable states. Spectroscopic data from Ref. [9] was used as an example for the temperature evaluation. The method suffers from uncertainties. The largest contribution comes from the uncertainty in the measurements of the ratios of spectral lines (5%), leading to 50% error in temperature measurement. Uncertainties in the densities of metastable states ( $\sim 20\%$ ) and optical cross-sections ( $\sim 30\%$ ) [12] were checked to be much less important. Moreover, uncertainty in the  $n_{1s_3}$  and  $n_{1s_5}$  can be improved by using tunable laser methods, e.g. laser absorption spectroscopy [15]. We also hope for the improvement of the accuracy of the cross-section measurements in future. Another possibility to improve the accuracy of the method is to use more different line ratios, which will help to localize the solution on  $(T_e^1, T_e^2)$  plane. Increasing the number of ratios involved may also allow to extend the method to non-Maxwellian multiple-parameter EEDFs and also to the relative measurements of the electron temperature.

This research was funded by Das Bundesministerium für Wirtschaft durch das Zentrum für Luft- und Raumfahrt e.V. (DLR) unter dem Förderkennzeichen 50 WB 0203.

1. V. N. Ochkina, *Spectroscopy of Low Temperature Plasma*, Wiley-WCH, Berlin, 2009.
2. R. J. Sovie, *Phys. Fluids* **7**, 613 (1963).
3. D. Samsonov and J. Goree, *IEEE Trans. Plasma Sci.* **27**, 76 (1999).
4. J. B. Boffard, C. C. Lin, and C. A. DeJoseph Jr., *J. Phys. D* **37**, R143 (2004).
5. N. J. Kang, S. Oh, and A. Ricard, *J. Phys. D* **41**, 155203 (2008).
6. X.-M. Zhu, W.-C. Chen, J. Li, and Y.-K. Pu, *J. Phys. D* **42**, 025203 (2009).
7. B. I. Moiseevitch and S. J. Smith, *Rev. Mod. Phys.* **40**, 238 (1968).
8. D. W. O. Heddle and J. W. Gallagher, *Rev. Mod. Phys.* **61**, 221 (1989).
9. S. Mitic, M. Y. Pustyl'nik, and G. E. Morfill, *New J. Phys.* **11**, 083020 (2009).
10. H. M. Thomas, G. E. Morfill, V. E. Fortov et al., *New J. Phys.* **10**, 033036 (2008).
11. J. B. Boffard, B. Chiaro, T. Weber, and C. C. Lin, *Atomic Data and Nuclear Data Tables* **93**, 831 (2007).
12. J. B. Boffard, G. A. Piech, M. F. Gehrke et al., *Phys. Rev. A* **59**, 2749 (1999).
13. Z. Gavare, D. Gött, A. V. Pipa et al., *Plasma Sources Sci. Technol.* **15**, 391 (2006).
14. F. E. Irons and J. Quant, *Spectrosc. Radiat. Transfer* **22**, 1 (1979).
15. H. T. Do, V. Sushkov, and R. Hippler, *New J. Phys.* **11**, 033020 (2009).